Optimized Diffuse Scattering Selection for Large Area Real-Time Geometry-Based Stochastic Modeling of Vehicular Communication Links

Benjamin Rainer[1], Markus Hofer[1], Laura Bernado[1], Stefan Zelenbaba[1], David Löschenbrand[1],
Dakic Anja[1], Thomas Zemen[1], Peter Priller[2], Xiaochun Ye[3], and Wenming Li[3]
[1]Austrian Institute of Technology GmbH, Giefinggasse 4, 1210 Vienna, Austria
[2]2 AVL List GmbH , Hans-List-Platz 1, 8020 Graz, Austria
[3]Institute of Computing Technology, CAS, China

Abstract—**In this paper we present a geometry-based stochastic channel model (GSCM) for mobile urban scenarios. GSCMs are very use case specific and high effort is needed to transfer existing ones to other scenarios. We propose to use OpenStreetMap data bootstrapping the geometry including the automatic placement of static, mobile and diffuse scatterers. We propose a method to distribute diffuse scatterers along buildings and roads. Our goal is to model complete city areas having the use case of real-time emulation of the wireless channel for vehicle-to-everything (V2X) communication in mind. In order to achieve this ambitious goal we propose a novel active scattering set selection based on locality-sensitive hashing (LSH). We show the trade-off between the number of selected diffuse scattering points by comparing the resulting power delay profile and Doppler spectral density to a measurement campaign.**

I. Introduction

Geometry-based stochastic channel models have been successfully applied to a variety of scenarios ranging from simple to highly mobile scenarios [1]. GSCMs use simplified ray tracing methods (e.g, 2D ray tracing, 2.5D ray tracing) and model the non line-of-sight components, such as those caused by diffuse scattering, penetration/refraction, and diffraction at edges by stochastic scatterers. The statistics of the scatterers' distributions are obtained by measurements. Due to the nature of GSCMs these models can be computed very fast, even satisfying the constraints for real-time channel emulation, recently shown in [2]. However, real-time capable GSCMs represent small areas with a low number of scatterers leading to a low accuracy.

An approach to reduce the computational complexity of diffuse scattering in GSCMs is presented in [3]. The complexity reduction of diffuse scattering has been mainly accomplished by the use of discrete prolate spheroidal sequences (DPSS) and their approximate basis coefficient calculation introduced in [4]. In [5] a GSCM for high speed railway is presented and the active scattering region (ASR) and geometry clusters are introduced. The introduced active scattering regions shall provide means to model the (diffuse) scattering from the environment within certain geometry clusters holding a certain type of scatterers. However, the parameters (e.g., life time/distance, size/shape, energy distribution) of such geometry clusters and ASRs are derived by a measurement.

The scenarios modeled with GSCMs and measured were rather limited in extend (e.g., short highway sections, simplified intersections, etc.). We provide a GSCM which is capable of simulating urban areas directly taken from OpenStreetMap in real-time. This includes automatic placement of diffuse scatterers along buildings, vegetation, tram rails and roads as well as the placement of static discrete scatterers which represent traffic signs, traffic lights and other objects. We further support the import of GPS trajectories for mobile discrete scatterers, receiver(s), and transmitter(s). Following this approach, a vast amount of diffuse scatterers are placed for even rather small inner-city areas. Therefore, we present an approach to restrict the number of active diffuse scatterers with only a minor impact on the obtained power delay profile (PDP) and Doppler spectral density (DSD). The scientific contributions of this paper are as follows:

- We present a GSCM which can be initialized using OpenStreetMap data.
- We formulate the search and selection of active diffuse scatterers as an approximate nearest neighbor problem and solve it using locality-sensitive hashing (LSH).
- We compare our GSCM with the active diffuse scattering selection to the results obtained from a measurement campaign.

II. Geometry-based stochastic channel model

In order to model urban areas, the correct representation of buildings and objects on and aside the road is a must. We speed up the tedious task of reconstructing the area of interest and placing diffuse, static, and mobile discrete scatterers as well as defining their movement. We use OpenStreetMap data to automatically import and instantiate our GSCM which is implemented using MATLAB. Besides buildings, roads, rail tracks, traffic lights/signs and vegetation, we also provide the possibility of importing GPS trajectories for defining the mobility of mobile discrete scatterers (e.g., cars, pedestrians, etc.), receivers and transmitters. If the GPS sampling rate is lower than the assumed stationarity region duratio [6] we interpolate

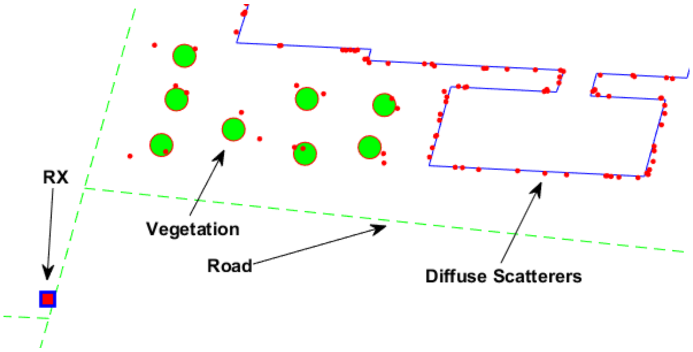

Fig. 1: Placement of different scatterers in the geometry imported from OpenStreetMap.

the trajectories using splines and the given stationarity duration as supporting points. This leads to a smoother time- and frequency-variant channel response. Fig. 1 depicts an example geometry, extracted from OpenStreetMap data. Metallic objects like traffic signs and lights are represented as static discrete scatterers. Vegetation is modeled by diffuse scatterers. We further allow to specify so-called diffuse scattering areas (polygons) where diffuse scatterers, parameterized with gain and path loss exponent, are distributed according to a given density parameter. We calculate a bounding box within which we uniformly distribute the diffuse scattering points. Finally, we delete all points, which do not fall in the specified polygon.

We uniformly distribute diffuse scattering points along the walls of each building. The distribution is parameterized by w_{D} denoting the maximum distance of diffuse scatterers to the nearest wall of the building, accounting for irregularities (windows, wall elements, etc.). We further introduce χ_{D} which denotes the density of diffuse scattering points on a single wall. Let $s := (x_1, y_1, x_2, y_2) \in \mathbb{R}^4$ be a line segment of a building's polygon. Then the exact number of diffuse scatterers along this line segment is given by

$$n_{\mathrm{D}} = \lceil ||(x_1, y_1) - (x_2, y_2)||_2 \cdot \chi_{\mathrm{D}} \rceil .$$

The n_D diffuse scattering points are then uniformly distributed in the rectangle given by $\boldsymbol{s}$ and w_D. For each diffuse scattering point we draw an uniformly distributed phase at the beginning of a simulation. In order to model diffraction we implement diffraction over rooftops as given in [7] and corner edge diffraction according to [8]. If vegetation blocks the line of sight between receiver and transmitter we calculate its' attenuation according to equation (2) in [9].

III. Active Scattering Selection

Problem 1: Let $P \subset \mathbb{R}^m$ with $|P| = n$, $Q \subset \mathbb{R}^m$ be a set of query points and $d : \mathbb{R}^m \times \mathbb{R}^m \to \mathbb{R}$ be a metric. We want to find a set G of at most M points where $G = \bigcap_{\boldsymbol{q} \in Q} \{\boldsymbol{p} \in P : \boldsymbol{q} \in B(\boldsymbol{p}, r)\}$ and $B(\boldsymbol{p}, r) := \{\boldsymbol{x} \in P \cup Q : d(\boldsymbol{p}, \boldsymbol{x}) < r\}$ and $r > 0$.

Problem 1 states our problem for a single time instant (which is also called point location in equal balls). We observe that the dimensionality of our data is $m = 2$ or $m = 3$ and $d(\boldsymbol{x}, \boldsymbol{y}) = ||\boldsymbol{x} - \boldsymbol{y}||_2$. In a static scenario it is well known that the search can be efficiently solved by using minimal spanning trees (MST). However, in our case the query point(s) move over time and even some diffuse scattering points may change their position (mobile scatterers). Thus, we would have to rebuild the MST for every time instant which takes $O(n \log n)$. Therefore, it is desirable that we build a data structure only once such that we have to recompute only the time-varying points. These thoughts instantly lead to hash functions. More specifically, in our case we need hash functions which are locality sensitive with respect to a metric according to Def. 3.1 [10].

Definition 3.1: A family $\mathcal{H} = h : S \to U$ of hash functions is called (r, cr, p_1, p_2)-sensitive for a metric $d : S \times S \to \mathbb{R}^+$ if $\forall v, q \in S$:

i) if $q \in B(v, r) \implies \mathbb{P}(h(v) = h(q)) \geq p_1 \; \forall h \in \mathcal{H}$,
ii) if $q \notin B(v, cr) \implies \mathbb{P}(h(v) = h(q)) \leq p_2 \; \forall h \in \mathcal{H}$.

A locality-sensitive hash (LSH) family is only useful if the probabilities satisfy $p_1 > p_2$ and the radius satisfies $r < cr$ which we establish by setting $c := 1 + \varepsilon$, $\varepsilon > 0$. In order to apply the LSH scheme presented in [10] we construct k hash functions $h(\boldsymbol{v}) := \left\lfloor \frac{<\boldsymbol{a},\boldsymbol{v}>+b}{r} \right\rfloor$ using the random projection principle where $\boldsymbol{a}$ is drawn from m independent standard normal distributions (which are $2-stable$), b is drawn from $U(0, r)$. The distance between $< \boldsymbol{a}, \boldsymbol{v} >$ and $< \boldsymbol{a}, \boldsymbol{q} >$ is distributed according to $\mathcal{N}(0, \frac{||\boldsymbol{v}-\boldsymbol{q}||_2^2}{r^2})$. Since we select k hash functions uniformly and independently, we observe from Def. 3.1 that all k hash functions have to collide which happens with probability greater or equal to p_1^k to fulfill (i).

Let P_{D} be the maximum path loss threshold for diffuse paths in dB. Then, we select the radius of the balls / buckets as $r := \frac{1}{2} 10^{-\frac{P_{\mathrm{D}}}{10 p_l}}$, where p_{l} denotes the path loss exponent for diffuse paths. This selection ensures that for any two points within $B(\boldsymbol{p}, r)$ the attenuation is no less than $2P_{\mathrm{D}}$, since for $\boldsymbol{v}, \boldsymbol{u} \in B(\boldsymbol{p}, r) : ||\boldsymbol{u} - \boldsymbol{v}||_2 \leq ||\boldsymbol{u} - \boldsymbol{p}||_2 + ||\boldsymbol{v} - \boldsymbol{p}||_2 < 2r$ by the Minkowski inequality. Please note, that our goal is not to find the nearest neighbor of certain query points, but to find all *ball centers* for which the given query points are contained within their respective r-balls. Thus, we proceed as described in [10], [11] by selecting L tables of such hash function sets with k hash functions and we define $g_i(\boldsymbol{v}) := (h_{i,1}(\boldsymbol{v}), \ldots, h_{i,k}(\boldsymbol{v}))$, $1 \leq i \leq L$. For a query point $\boldsymbol{q}$ we lookup $g_1(\boldsymbol{q}), \ldots, g_L(\boldsymbol{q})$ and stop searching after we have encountered $\leq 3L$ points. If an encountered point $v_j \in B(\boldsymbol{q}, cr)$ then we return the point. We set $L = \frac{M}{3}$ and $k = 10$ such that with constant probability it holds that if $u \in B(\boldsymbol{q}, r)$ then there $\exists i \in \{1, \ldots, L\}$: $g_i(\boldsymbol{q}) = g_i(\boldsymbol{u})$ and $\sum_{j=1}^{L} |(P \setminus B(\boldsymbol{q}, cr)) \cap g_j^{-1}(g_j(\boldsymbol{q}))| < 3L$ (guarantees correctness).

Let f be the density of our absolute standard normal distributed random variable and with transforming $x = cy$ we have

$$p(c) = \mathbb{P}(h_{\boldsymbol{a},b}(\boldsymbol{v}) = h_{\boldsymbol{a},b}(\boldsymbol{q})) = \int_0^r \frac{1}{c} f\left(\frac{x}{c}\right)\left(1 - \frac{x}{r}\right) dx.$$

By our selection, r is fixed and with $c = \frac{||\boldsymbol{v}-\boldsymbol{q}||_2}{r}$ it is easy to see that our selection fulfills Def. 3.1 (i) and (ii) for $p_1 =$

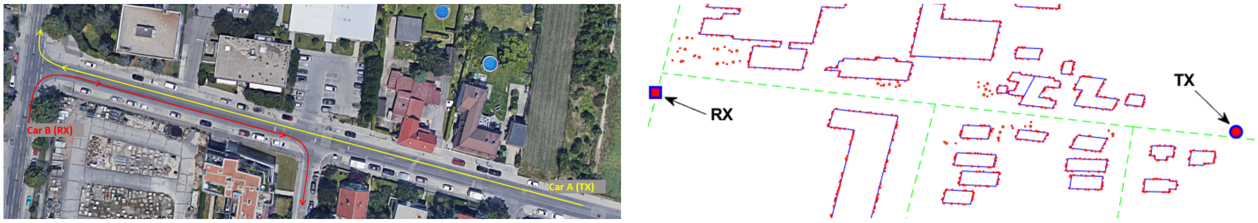

(a) Scenario of the measurement campaign (©Google).

(b) Reconstructed scenario from OpenStreetMap and GPS data with diffuse scatterers automatically placed.

Fig. 2: Measurement scenario including the trajectories for the transmitter, receiver and the geometry.

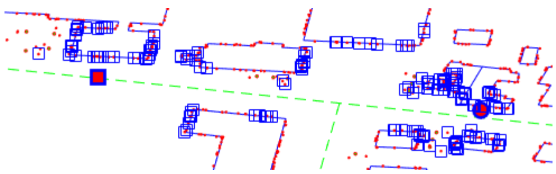

Fig. 3: Selection of diffuse scatterers during simulation for a single time instant, highlighted by blue rectangles.

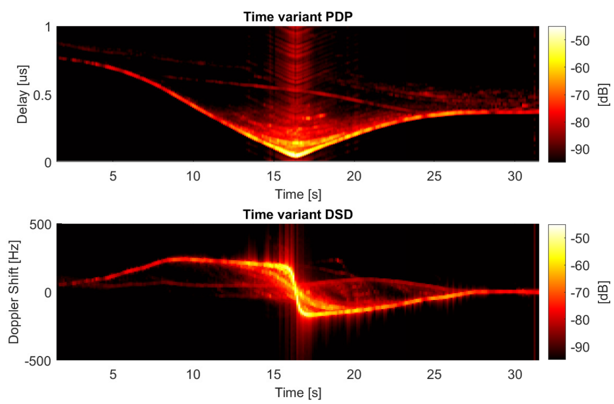

Fig. 4: PDP and DSD of the measurement campaign.

$p(1)$ and $p_2 = p(1+\varepsilon)$ (with increasing distance of $\boldsymbol{q}$ and $\boldsymbol{v}$ the collision probability monotonically decreases). We further omit the correctness check ($\boldsymbol{v} \in B(q, cr)$) after obtaining a list of possible diffuse scattering points because we check whether the selected diffuse scattering points are within the line-of-sight of the receiver and transmitter, respectively and whether the inclusion condition is fulfilled such that we obtain our set G.

IV. Measurement Campaign and Comparison to Simulation

In order to assess how well our GSCM with the proposed active diffuse scattering selection is able to reproduce measurements, we compare the results to a measurement campaign conducted in Vienna ($48°16'04.9''$N $16°25'56.6''$E). The measurement is conducted using the AIT multi-node channel sounder [12] with a bandwidth of $B = 150$ MHz at a center frequency of 3.5 GHz. The sub-carrier spacing is $\Delta f = 250$ kHz and the snapshot interval is 500 μs. The scenario of the measurement campaign is provided in Fig. 2. The antennas are mounted on the transmitting node on a Toyota Prius at a height

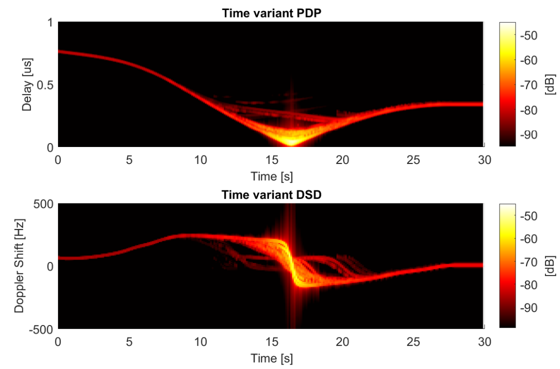

Fig. 5: PDP and DSD obtained by the GSCM selecting 300 active diffuse scattering points for each stationarity region.

of approximately 1.4 m. For the receiving node we mount the antenna on a Volkswagen T5 at a height of 2 m. The speed of the cars varies between 0 km/h and 40 km/h. We use $\lambda/2$ dipole antennas for the measurement and the simulation. The trajectories for the transmitter and receiver are collected during measurement, having a GPS sampling rate of 1Hz. Thus, we assume a constant velocity between two sampling points. We interpolate the obtained GPS trajectories using splines, where we use the sampled GPS points as supporting points and interpolate points that are spaced according to the assumed stationarity region duration.

For the simulation scenario we do not model the parked cars along the streets and we do not model other mobile vehicles in the scenario. Our goal is to investigate how the proposed selection of diffuse scatterers does perform in the PDP and DSD. We use the OpenStreetMap data as it is provided online. For the placement of diffuse scatterers and for obtaining the bucket width for LSH, we set $\chi_{\mathrm{D}} = 0.5$, $w_{\mathrm{D}} = 0.5$, $P_{\mathrm{D}} = -90$ dB and the path loss exponent for diffuse paths to $p_{\mathrm{l}} = 5.0$. We further set $M = 300$ which yields at most 300 diffuse scattering paths. For the query points we use the transmitter position (TX), the receiver position (RX) and $\boldsymbol{q} = \mathrm{TX} + \frac{\mathrm{RX}-\mathrm{TX}}{2}$. Fig. 3 depicts the selection of diffuse scattering points for a single time instant during simulation before the line-of-sight check. In total we have 1536 diffuse scattering points distributed along the buildings.

We estimate the local scattering function (LSF) from the gathered discrete time- and frequency-varying channel trans-

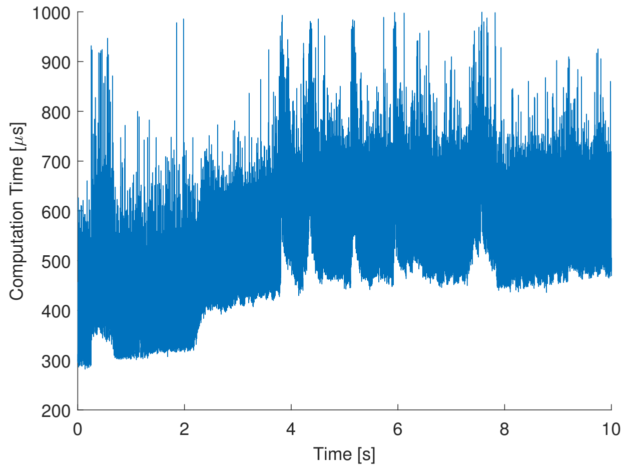

Fig. 6: CPU time needed calculating the channel response.

fer function (measurement and simulation) $h[m, q]$ according to [13] using a multi-taper estimate with I orthogonal time-domain and J orthogonal frequency-domain tapers. We collect S samples in time and $Q = 601$ samples in frequency per snapshot. The stationarity region is indexed in time by $k_\mathrm{t} \in \{1, \ldots, \lfloor S/M \rfloor\}$ and in frequency by $k_\mathrm{f} \in \{1, \ldots, \lfloor Q/N \rfloor\}$ resulting in a region size of $M \times N$. For the measurement and simulation we use a stationarity time $t_s = 0.12$ s [6] and a stationarity bandwidth of $f_\mathrm{stat} = 150$ MHz. The time-varying PDP and DSD can be defined as the marginals of the LSF on the delay and Doppler axis, respectively.

The PDP and DSD of the measurement campaign are presented in fig. 4. We observe a path that has zero Doppler. This path is a reflection from a metallic object behind the receiver which has not been modeled in the simulation. Fig. 5 depicts the PDP and DSD for the simulation using our proposed selection of active diffuse scatterers. The DSD shows that even with such a small amount of $M = 300$ scatterers we are able to reproduce the diffuse paths to a certain extent. We obtain a good match when receiver and transmitter are near. However, beginning at second 15 we encounter diffuse paths which are not present in the measurement. The reason are the missing object besides the streets such as big trees (which are not present in the OpenStreetMap data, cf. fig. 2a).

In order to assess the simulation speed of IEEE 802.11p V2X communication we set the stationarity duration to 1 ms, the bandwidth to 10 MHz, a carrier frequency of 5.9 GHz and 64 subcarriers. We evaluate the performance on an Intel(R) Xeon(R) Gold 6150 CPU with 2.70 GHz for a duration of 10 s. The selection of the diffuse scatterers takes at most 0.012 s including the intersection checks. In order to be real-time capable we compute the diffuse scatterers in parallel which results in diffuse scattering set updates approximately every 15 stationarity regions. In our scenario this corresponds to a traveled distance of approx. 0.15 m. Fig 6 depicts the time needed for calculating the power and the projection using DPSSs.

V. Conclusion

In this paper we present a GSCM for urban areas that can be created with low effort. It reads data directly from OpenStreetMaps and places scatterers automatically in the scenario. The trajectories of mobile vehicles or entities can be defined by using any OpenStreetMap editor. The parameters of the GSCM can be provided in the OpenStreetMap data. The proposed active (diffuse) scatterer selection allows for real-time simulation and is thus appropriate to be used as channel model for real-time emulations in large geographical areas.

VI. Acknowledgments

This work is funded by the Austrian Research Promotion Agency (FFG) and the Austrian Ministry for Transport, Innovation and Technology (bmvit) within the project REALISM (864188) of the funding program transnational projects.

References

[1] J. Karedal, F. Tufvesson, N. Czink, A. Paier, C. Dumard, T. Zemen, C. F. Mecklenbrauker, and A. F. Molisch, "A geometry-based stochastic mimo model for vehicle-to-vehicle communications," *IEEE Transactions on Wireless Communications*, vol. 8, no. 7, pp. 3646–3657, July 2009.

[2] M. Hofer, Z. Xu, D. Vlastaras, B. Schrenk, D. Loschenbrand, F. Tufvesson, and T. Zemen, "Real-time geometry-based wireless channel emulation," *IEEE Transactions on Vehicular Technology*, pp. 1–1, 12 2018.

[3] N. Czink, F. Kaltenberger, Y. Zhou, L. Bernadó, T. Zemen, and X. Yin, "Low-complexity geometry-based modeling of diffuse scattering," in *Proceedings of the Fourth European Conference on Antennas and Propagation*, April 2010, pp. 1–4.

[4] F. Kaltenberger, G. Steinbock, G. Humer, and T. Zemen, "Low-complexity geometry based mimo channel emulation," in *First European Conference on Antennas and Propagation*, Nov 2006, pp. 1–8.

[5] L. Zhou, F. Luan, S. Zhou, A. F. Molisch, and F. Tufvesson, "Geometry-based stochastic channel model for high-speed railway communications," *IEEE Transactions on Vehicular Technology*, vol. 68, no. 5, pp. 4353–4366, May 2019.

[6] L. Bernadó, T. Zemen, F. Tufvesson, A. F. Molisch, and C. F. Mecklenbräuker, "The (in-) validity of the wssus assumption in vehicular radio channels," in *2012 IEEE 23rd International Symposium on Personal, Indoor and Mobile Radio Communications*, Sep. 2012, pp. 1757–1762.

[7] ITU, "ITU-R p.526: Propagation by diffraction." Tech. Rep., 2019.

[8] L. Raschkowski, P. Kyösti, K. Kusume, T. Jämsä, V. Nurmela, A. Karttunen, A. Roivainen, T. Imai, J. Järveläinen, J. Medbo, J. Vihriälä, J. Meinilä, K. Haneda, V. Hovinen, J. Ylitalo, N. Omaki, A. Hekkala, R. Weiler, and M. Peter, "Metis channel models (d1.4)," 07 2015.

[9] A. S. Adegoke, D. A. T. Siddle, and S. O. Salami, "Vegetation attenuation and its dependence on foliage density," 2016.

[10] M. Datar, N. Immorlica, P. Indyk, and V. S. Mirrokni, "Locality-sensitive hashing scheme based on p-stable distributions," in *Proceedings of the Twentieth Annual Symposium on Computational Geometry*, ser. SCG '04. New York, NY, USA: Association for Computing Machinery, 2004, p. 253–262. [Online]. Available: https://doi.org/10.1145/997817.997857

[11] P. Indyk and R. Motwani, "Approximate nearest neighbors: Towards removing the curse of dimensionality," in *Proceedings of the Thirtieth Annual ACM Symposium on Theory of Computing*, ser. STOC '98. New York, NY, USA: Association for Computing Machinery, 1998, p. 604–613. [Online]. Available: https://doi.org/10.1145/276698.276876

[12] S. Zelenbaba, D. Loeschenbrand, M. Hofer, A. Dakic, B. Rainer, G. Humer, and T. Zemen, "A scalable mobile multi-node channel sounder," *IEEE Wireless Communications and Networking Conference*, pp. 1–5, April 2020.

[13] L. Bernado, T. Zemen, A. Paier, J. Karedal, and B. H. Fleury, "Parametrization of the local scattering function estimator for vehicular-to-vehicular channels," in *2009 IEEE 70th Vehicular Technology Conference Fall*, Sep. 2009, pp. 1–5.